# Secreting and Sensing the Same Molecule Allows Cells to Achieve Versatile Social Behaviors

Hyun Youk and Wendell A. Lim*

READ THE FULL ARTICLE ONLINE
http://dx.doi.org/10.1126/science.1242782

Cite this article as H. Youk, W. A. Lim, *Science* **343**, 1242782 (2014).
DOI: 10.1126/science.1242782

**Introduction:** Cells that simultaneously secrete and sense the same signaling molecule are ubiquitous. Bacteria sense a quorum by secreting and sensing an autoinducer; T cells induce a monoclonal immune response by secreting and sensing a cytokine; and epithelial cells can become cancerous through misregulated secreting and sensing of a growth factor. Many of these cells use the same core signaling-circuit motif to realize a diverse repertoire of biological functions. The full range of functions that the "secrete-and-sense" circuit motif can achieve, and the design principles underlying its functional flexibility, remain poorly understood.

**Methods:** We constructed a synthetic secrete-and-sense circuit motif in budding yeast that enabled the yeast to secrete and sense the mating pheromone. We systematically altered key parameters of the circuit—secretion rate, receptor abundance, positive feedback linking sensing with secretion, and signal degradation—to reveal how they enabled various cellular behaviors. Through single-cell measurements, we assessed the degree to which a secrete-and-sense cell responded to its own secreted signal (self-communication) versus the signal secreted by its neighbors (neighbor communication) to achieve diverse cellular behaviors.

**Results:** We show that the core secrete-and-sense circuit motif can precisely tune the cell's "sociability"—the cell's degree of self- versus neighbor communication—using one molecule and receptor pair. At the extremes, the circuit enables purely social behaviors (e.g., quorum sensing) in which cells mainly use neighbor communication, or purely asocial behaviors (e.g., epidermal growth factor signaling in epithelial cells) in which cells mainly use self-communication, commonly referred to as "autocrine signaling." Crucially, we uncover rich behaviors that rely on simultaneous self- and neighbor communication, including some that have been observed in nature but whose mechanistic origins have been unclear. For example, positive feedback that links sensing with secretion can yield a bistable behavior in which all cells in the population act as an ensemble to be either quiescent or maximally activated. Incorporation of an active signal degradation enables bimodal activation, in which the different proportions of the population bifurcate into distinct activation states, with the ratio of the two states determined by simultaneous self- and neighbor communication. This behavior explains how isogenic cells can differentiate into distinct states with defined ratios.

**Discussion:** We integrate simple models, single-cell measurements, and a bottom-up synthetic biology approach to reveal a range of population-level behaviors that arise from the core secrete-and-sense circuit motif. We determine how the intracellular circuit elements result in distinct classes of self- and neighbor communication, and in turn leads to various population-level behaviors. Our work reveals "phase diagrams" that summarize the relationship between the circuit architecture and different phases of population-level behaviors for the secrete-and-sense circuit. Our first-principles approach may be generalized to reveal relationships between the structures of other fundamental cell-signaling circuits and the multicellular behaviors that they enable.

## FIGURES AND TABLES IN THE FULL ARTICLE



## SUPPLEMENTARY MATERIALS



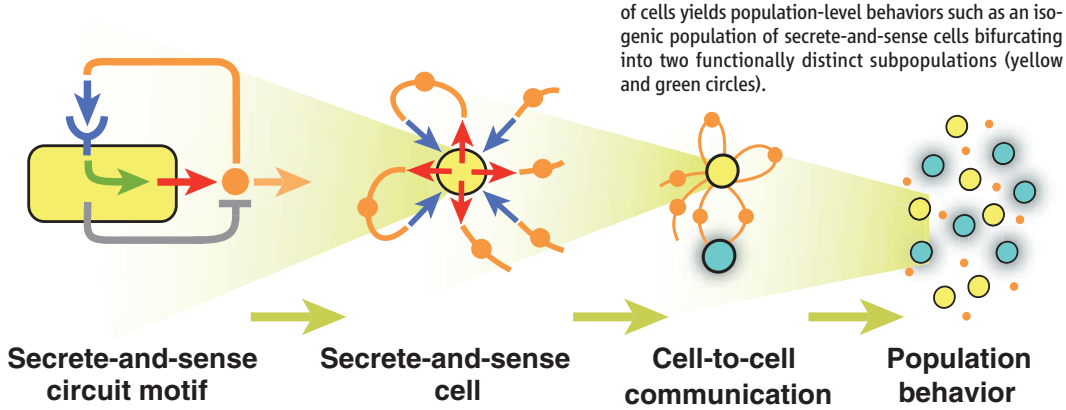


**From circuits to multicellular behaviors: a bottom-up synthesis of hierarchy.** The secrete-and-sense circuit controls how each cell (yellow circle) communicates through a signaling molecule (orange circle), which in turn controls the cell-to-cell communication. The collection of cell-to-cell communication in all pairs of cells yields population-level behaviors such as an isogenic population of secrete-and-sense cells bifurcating into two functionally distinct subpopulations (yellow and green circles).

The list of author affiliations is available in the full article online.
*Corresponding author. E-mail: lim@cmp.ucsf.edu

# Secreting and Sensing the Same Molecule Allows Cells to Achieve Versatile Social Behaviors

Hyun Youk[1,2] and Wendell A. Lim[1,2,3]*

Cells that secrete and sense the same signaling molecule are ubiquitous. To uncover the functional capabilities of the core "secrete-and-sense" circuit motif shared by these cells, we engineered yeast to secrete and sense the mating pheromone. Perturbing each circuit element revealed parameters that control the degree to which the cell communicated with itself versus with its neighbors. This tunable interplay of self-communication and neighbor communication enables cells to span a diverse repertoire of cellular behaviors. These include a cell being asocial by responding only to itself and social through quorum sensing, and an isogenic population of cells splitting into social and asocial subpopulations. A mathematical model explained these behaviors. The versatility of the secrete-and-sense circuit motif may explain its recurrence across species.

A central goal of systems biology is to understand how various cells use the common small repertoire of circuit elements to communicate with each other to achieve diverse functions (*1*–*19*). Of particular interest is the class of circuits that are found in cells that simultaneously secrete and sense the same extracellular molecule (Fig. 1A) because it is ubiquitous across species. Examples of such cells include (Fig. 1B) bacteria that secrete and sense the autoinducers for quorum sensing (*20*–*37*), human pancreatic β cells that secrete and sense insulin (*38*, *39*), vulva precursor cells in *Caenorhabditis elegans* that secrete and sense the diffusible Delta (*40*–*44*), and human T cells that secrete and sense the cytokine interleukin-2 (IL-2) to regulate their growth (*45*–*49*). In some cases, a cell that secretes and senses the same molecule communicates with itself ("self-communication") but not with its neighboring cells, whereas in other cases such a cell communicates with its neighboring cells ("neighbor communication") but not with itself. Moreover, in some cases, the secrete-and-sense cell communicates both with itself and with its neighbors (Fig. 1C). The advantages of using secrete-and-sense circuits have been unclear in many situations. For example, if a cell's primary purpose is self-communication, then it is unclear why the cell secretes a molecule instead of relying entirely on intracellular signaling. To address these questions, we experimentally explored the full functional capabilities of the secrete-and-sense circuits that arise from the interaction between self-communication and neighbor communication. We sought common design principles that tie together the seemingly disparate examples of secrete-and-sense circuits. We used the budding yeast's mating pathway as a model system in which we could systematically modify the secrete-and-sense circuits to determine what features affect the degree of self-communication versus neighbor communication. We demonstrate that varying the key parameters of the secrete-and-sense circuits allows cells to achieve diverse classes of behaviors, thus suggesting that secrete-and-sense circuits' functional flexibility may explain its recurrence throughout nature.

[1]Department of Cellular and Molecular Pharmacology, University of California, San Francisco, San Francisco, CA 94158, USA. [2]Center for Systems and Synthetic Biology, University of California, San Francisco, San Francisco, CA 94158, USA. [3]Howard Hughes Medical Institute, University of California, San Francisco, San Francisco, CA 94158, USA.

*Corresponding author. E-mail: lim@cmp.ucsf.edu

## Results

### Basic Secrete-and-Sense Circuit in Yeast

Our model "secrete-and-sense system" is the haploid budding yeast that has been engineered to secrete and sense the mating pheromone α-factor (*50*–*60*) (Fig. 1D). The cell senses the α-factor through its membrane receptor Ste2 and responds by expressing the green fluorescent protein (GFP) through the α-factor–responsive promoter *pFUS1* (Fig. 1D and fig. S1) (*51*). The cell increases GFP expression as the concentration of the exogenous α-factor increases. We used a *far1*Δ strain that did not arrest its cell cycle or mate upon stimulation by α-factor.

### Disentangling Effects of Self-Communication and Neighbor Communication

To establish whether the cell's response to sensing the molecule that it secreted (self-communication) could be distinguished from its response to the same molecule that had been secreted by its neighboring cells (neighbor communication), we designed an experiment in which we cultured our secrete-and-sense strain with another strain, called the "sense-only" strain, which senses but does not secrete α-factor (Fig. 2A). The sense-only strain could only respond to the α-factor secreted by the secrete-and-sense strain. On the other hand, a secrete-and-sense cell could potentially respond to both the α-factor that it secreted (self-communication) and the α-factor secreted by the other secrete-and-sense cells in the same batch liquid culture environment (neighbor communication). Thus, we reasoned that if we detected any difference between the reporter GFP level of the secrete-and-sense strain (referred as cell A throughout Fig. 2) and that of the sense-only strain (referred as cell B throughout Fig. 2), then we could ascribe such effects to self-communication.

### Construction of Library of Secrete-and-Sense Strains

We constructed a set of secrete-and-sense strains (Fig. 2B) and a set of sense-only strains (strain list in table S1). In each secrete-and-sense strain, doxycycline-inducible promoter *pTET07* expressed the *MFα1* gene that encodes α-factor (*MATa*; *bar1*Δ *far1*Δ) (Fig. 2B and fig. S2). Doxycycline, a small molecule that readily diffused into the cell to control gene expression through the promoter *pTET07*, was used to tune the secretion rate of the α-factor. Increasing concentration of doxycycline caused an increasing expression of the genes under the control of *pTET07*. The GFP expression was controlled by the promoter *pFUS1* that is induced by the α-factor (fig. S1) (*51*). We constructed various secrete-and-sense strains by varying the promoter that expressed Ste2. For each secrete-and-sense strain, we constructed an analogous sense-only strain that lacked the *MFα1* gene. Each sense-only strain also constitutively expressed the fluorescent protein mCherry, which the secrete-and-sense strains lacked. This allowed us to use a flow cytometer to distinguish the sense-only strains from the secrete-and-sense strains when they were cultured together.

### Experimental Demonstration of Self-Communication

We cultured our basic secrete-and-sense strain with its partner basic sense-only strain. Both of these "basic" strains had the same endogenous promoter *pSTE2* controlling expression of the Ste2 receptor (fig. S3). We grew these strains together at equal initial cell densities in 5 ml of liquid medium in which we maintained a constant concentration of doxycycline. We used a flow cytometer to measure each strain's mean single-cell GFP fluorescence during the time course. We cultured these strains at various total cell densities [optical densities (ODs)] and doxycycline concentrations (figs. S4 to S7). When both the initial total cell density and the doxycycline concentration were low (for example, OD = 0.001, [doxycycline] = 6 μg/ml; Fig. 2C, left panel), the mean GFP fluorescence of the basic secrete-and-sense strain (cell A in Fig. 2C, left panel) swiftly increased then plateaued, whereas the mean GFP fluorescence of the basic sense-only strain (cell B in Fig. 2C, left panel) stayed at a basal value throughout the time course. This shows that each basic secrete-and-sense cell sensed and responded to the α-factor

that it secreted, whereas the amount of α-factor shared between cells (including between any two basic secrete-and-sense cells) was too low to activate the mating pathway. Thus, each basic secrete-and-sense cell self-communicated in this regime of low cell density and secretion rate. In cultures with the same initial total cell density but with a higher doxycycline concentration (OD = 0.001, [doxycycline] = 30 μg/ml; Fig. 2C, right panel), the basic secrete-and-sense strain's GFP fluorescence again swiftly increased to a higher plateau than it did in the culture with the lower production of α-factor (that is, compare cell A in both panels of Fig. 2C). GFP fluorescence of the basic sense-only strain also increased over time, albeit more slowly than that of the basic secrete-and-sense strain. Thus, increasing the secretion rate increased the degree of neighbor communication (including between different secrete-and-sense cells). The discrepancy between the amounts of GFP fluorescence of the two strains indicates that each basic secrete-and-sense cell, in addition to communicating with its neighbors, also self-communicates by sensing and responding to the higher concentration of its own secreted α-factor. If there were no self-communication, both strains would have the same GFP fluorescence.

We examined cultures of the two basic strains at a 100-fold higher total cell density (OD = 0.1; Fig. 2D). In the high cell density coculture with a low doxycycline concentration ([doxycycline] = 6 μg/ml; Fig. 2D, left panel), the basic sense-only strain's GFP fluorescence increased faster and to higher values than it did in the coculture with the same doxycycline concentration but with the lower cell density (that is, compared to cell B in Fig. 2C, left panel). Thus, the greater cell density caused the degree of neighbor communication to increase. The change in cell density did not affect the basic secrete-and-sense strain's self-communication because the cell density does not affect its secretion rate of α-factor per cell, which is the main determinant of the degree of self-communication for the basic secrete-and-sense strain. In cultures with a high total cell density and a high secretion rate (OD = 0.1, [doxycycline] = 30 μg/ml; Fig. 2D, right panel), there was virtually no difference in GFP fluorescence between the two strains. Hence, in these cultures, neighbor communication was dominant.

Together, our coculture experiments (Fig. 2, C and D) emphasize that self-communication and neighbor communication, despite both using the same signaling molecule, do not always lead to the same behavior over time in a cell that secretes and senses the same molecule. In general, the dynamics of the cell's response to a signal depends not just on the type of the signaling molecule being sensed but also on how the concentration of that molecule changes over time, and distinct dynamics of the same signaling pathway over time can lead to distinct cell fates (*17*). We developed a mathematical model that showed that the secrete-and-sense cell's response to self-communication and neighbor communication yields distinct dynamical responses because of the fact that the two modes of communication involve different time scales (*61*). Our model also explains the main features of our culture experiments and quantifies the degree of self-communication and neighbor communication (*61*).

### *High Receptor Expression and Secretion Rate Enhance Self-Communication*

We examined how varying the amount of the α-factor receptor Ste2 affected the degrees of self-communication and of neighbor communication. To do so, we repeated above experiments with strains that varied in the amount of Ste2 expressed (Fig. 2B, strains in table S1). In each pair, the secrete-and-sense and the sense-only strains used the same constitutive promoter to express Ste2 (figs. S8 and S9). We cultured each pair of strains as low cell density cultures (OD = 0.001; Fig. 2E), as high cell density cultures (OD = 0.1; Fig. 2F), and in a wide range of doxycycline concentrations. We used a flow cytometer to measure the mean single-cell GFP fluorescence of each strain after culturing each pair of strains for 5 hours in doxycycline together. By subtracting the mean single-cell GFP fluorescence of the sense-only strain (cell B) from that of the secrete-and-sense strain (cell A), for each of the seven pairs of strains in 11 different concentrations of doxycycline, we obtained "heat maps" for low cell density (OD = 0.001 for both strains; Fig. 2E) and high cell density (OD = 0.1 for both strains; Fig. 2F) cultures. The color of each pixel in the heat maps (of 7 × 11 pixels) represents the difference in the mean single-cell GFP fluorescence of the two strains for each culture condition.

The heat map for low cell density (Fig. 2E) showed combinations of receptor abundance and secretion rate that enabled the secrete-and-sense cells to self-communicate, and those that did not allow for self-communication. Specifically, in the region of the heat map defined by high secretion rates ([doxycycline] > 0.6 μg/ml) and high receptor expression values (top right quadrant in Fig. 2E), secrete-and-sense cells had higher GFP fluorescence than their counterpart sense-only cells

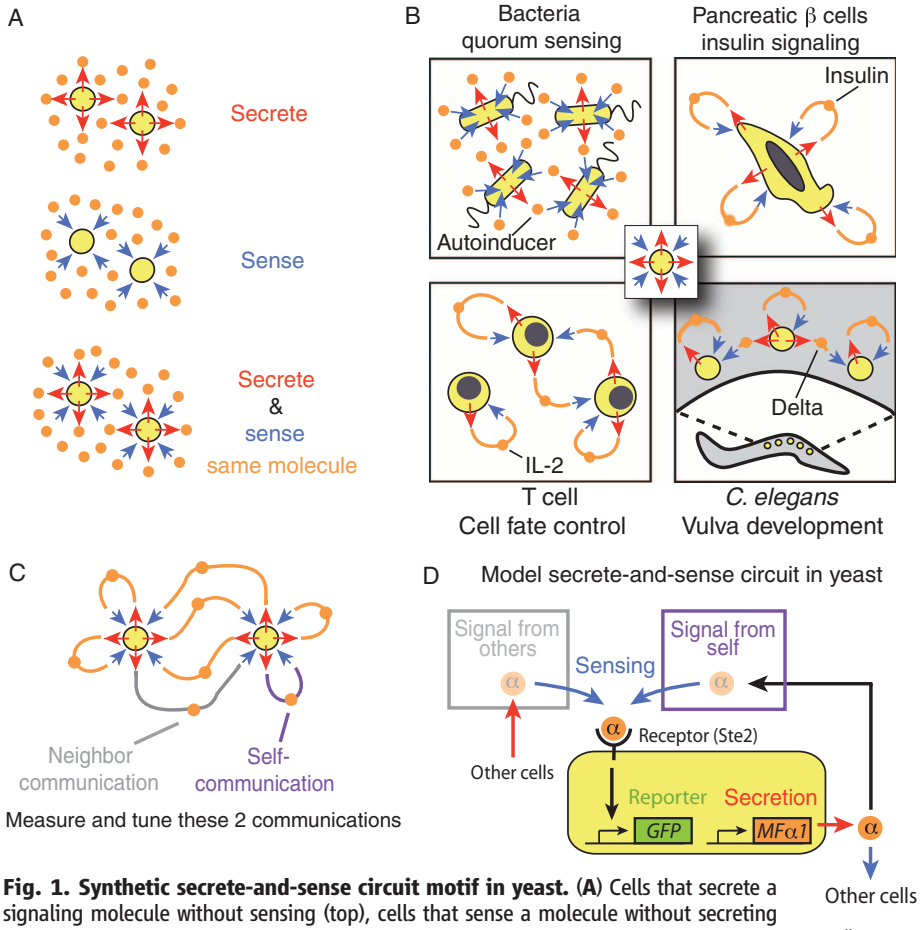


**Fig. 1. Synthetic secrete-and-sense circuit motif in yeast.** (**A**) Cells that secrete a signaling molecule without sensing (top), cells that sense a molecule without secreting (middle), and cells that secrete and sense the same signaling molecule (bottom). (**B**) Examples of "secrete-and-sense" cells in nature: bacteria secrete and sense an autoinducer for sensing a quorum, human pancreatic β cells secrete and sense insulin, human T cells secrete and sense the cytokine IL-2 to control their proliferation, and the vulva precursor cells in *C. elegans* secrete and sense the diffusible Delta for specifying their cell fates. (**C**) Schematic of self-communication and neighbor communication between two identical secrete-and-sense cells. (**D**) Schematic of synthetic secrete-and-sense system: haploid budding yeast (yellow box) engineered to secrete and sense α-factor (orange circle). GFP fluorescence is a readout of the concentration of α-factor sensed by the cell.

whose GFP fluorescence remained near basal values (*61*). This indicates that a secrete-and-sense cell with a high secretion rate and a high receptor expression is an "asocial" cell that self-communicates by efficiently capturing its own α-factor because of its highly abundant receptors. The secrete-and-sense cells with high secretion rates ([doxycycline] > 0.6 μg/ml) and lower range of receptor expression values (lower right quadrant of the heat map in Fig. 2E) had nearly the same GFP fluorescence values as their counterpart sense-only cells. This indicates that a secrete-and-sense cell with a low receptor expression and high secretion rate is a "social" cell that is unable to self-communicate because its receptor abundance is too low to capture its own α-factor for activating its mating pathway, but is ideal for communicating with its neighbors because of its high secretion rate (*61*). The secrete-and-sense cells with low secretion rate ([doxycycline] < 0.6 μg/ml; the left half of heat map in Fig. 2E), including those with high receptor abundances, had nearly the same GFP fluorescence as their counterpart sense-only cells. This indicates that these secrete-and-sense cells cannot self-communicate because they do not secrete enough α-factor, leading to negligible self-communication and neighbor communication in low cell density. The heat map for high cell density (Fig. 2F) showed that secrete-and-sense cells and sense-only cells had nearly identical GFP fluorescence at all secretion rate and receptor expression values once they had grown together for a sufficiently long time. This indicates that increasing the density of secrete-and-sense cells increases the neighbor communication because of the increased total population-level secretion of α-factor.

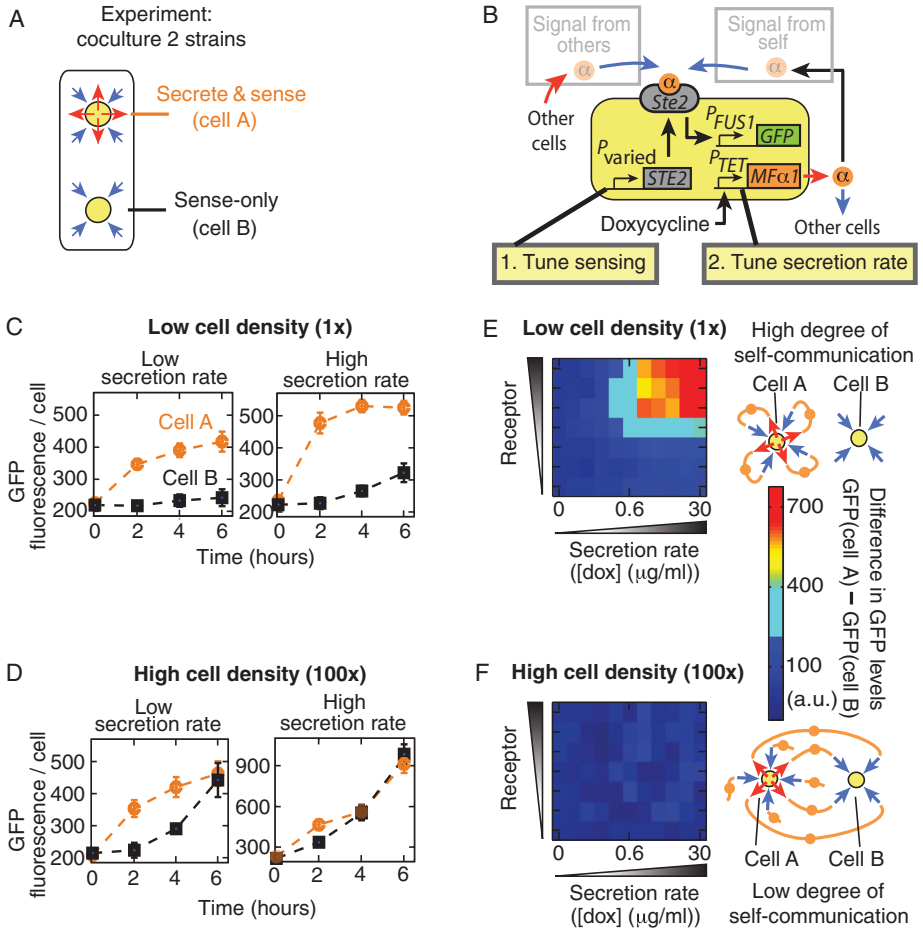


**Fig. 2. Varying receptor abundance and secretion rate to tune degrees of self-communication and neighbor communication.** (**A**) Secrete-and-sense strain ("cell A") and sense-only strain ("cell B") were cultured together for all experiments in this figure. (**B**) Each secrete-and-sense strain used a different promoter $P_{varied}$ to express *STE2*, but all used the *pTET07* to express *MFα1*. For each secrete-and-sense strain, a matching sense-only strain with the same Ste2 abundance was constructed. (**C** and **D**) Equal densities of "basic secrete-and-sense strain" and "basic sense-only strain" were cultured together for two representative doxycycline concentrations {[doxycycline] = 6 μg/ml ("low secretion rate") and 30 μg/ml ("high secretion rate")} and at two total cell densities [(C) low (OD = 0.001) and (D) high (OD = 0.1)]. Each strain's single-cell GFP fluorescence at various time points is shown. Error bars, SEM ($n$ = 3). (**E** and **F**) Each secrete-and-sense strain (cell A) was cultured with its partner sense-only strain (cell B) (that is, Ste2 expressed by the same promoter in both strains). Seven such pairs of strains were cultured for 5 hours in 11 different concentrations of doxycycline (dox) (table S1 and fig. S8), yielding heat maps with 7 × 11 pixels for (E) low (OD = 0.001) and (F) high (OD = 0.1) cell densities. Each pixel represents the difference between the GFP fluorescence of cell A and of cell B at the end of the time course (subtracting GFP fluorescence of cell B from that of cell A, averaged from three independent experiments).

### *Positive Feedback on Self-Communication and Neighbor Communication Enables Binary Cell Fates*

We next examined how the secrete-and-sense cell's degree of sociability could be further modulated by two regulatory mechanisms that are ubiquitous in naturally occurring secrete-and-sense circuits: positive feedback link (detection of the molecule leads to increased secretion of the molecule) (*62*–*64*) and active degradation of the signaling molecule (for example, secretion of a protease) (*20*).

We first investigated the influence of self-communication and neighbor communication on the positive feedback link. To the basic secrete-and-sense circuit (used in Fig. 2, B and C), we added a positive feedback link (highlighted in blue, Fig. 3A) in which production of α-factor was induced by the mating pathway by linking the *rtTA* expression by the promoter *pFUS1* and having the promoter *pTET07* expressing *MFα1*. We engineered this synthetic positive feedback link so that its strength could be tuned by increasing the doxycycline concentration (fig. S10). We cultured this positive feedback–equipped secrete-and-sense strain by itself in a wide range of doxycycline concentrations and at various cell densities. For each condition, we used a flow cytometer to obtain the histograms of mean single-cell GFP fluorescence at various time points (Fig. 3, B and C, and figs. S11 and S12). When the cell density was low (OD = 0.001) and the positive feedback was weak (for example, [doxycycline] = 3 μg/ml), this strain's GFP fluorescence remained at basal values throughout the time course (Fig. 3B, left column). This corresponds to an "OFF state" in which the cell secretes the α-factor at a low basal rate (indicated by its low basal GFP fluorescence). When positive feedback was strong in cultures of low cell density (for example, [doxycycline] = 40 μg/ml; Fig. 3B, right column), cells, which were initially in the OFF state, increased their signal response over time (corresponding to increasing its signal secretion rate) and, after 8 hours, reached a maximally allowed response—the "ON state"—in which cells secreted α-factor at the maximal possible rate (Fig. 3B, right column, and fig. S11). Thus, positive feedback enabled the initially quiescent secrete-and-sense cell to be "activated" to become maximally secreting cells. This behavior occurs in many natural secrete-and-sense cells with a similar positive feedback link (for example, cytokine signaling in T cells) (*47*, *48*, *62*, *63*, *65*–*68*).

At a high cell density (OD = 0.1), if the positive feedback was weak (for example, [doxycycline] = 3 μg/ml; Fig. 3C, left column), the cells activated, whereas they remained in the OFF state

in cultures of lower cell density with the same doxycycline concentration (Fig. 3B, left column) (fig. S12). This indicates that increased neighbor communication, through the population's collective amplification of the basal level secretion from each cell, probably accounts for this activation (Fig. 3C, left column).

To address whether these activation properties were primarily due to self-communication or neighbor communication, we incubated the positive feedback–equipped basic secrete-and-sense strain (Fig. 3A) with the analogous sense-only strain (characterized in fig. S10) under various doxycycline and cell density conditions (fig. S13). At low total cell density (OD = 0.001), the sense-only strain's GFP fluorescence initially remained at the basal values at the onset of the activation of the secrete-and-sense strain at all doxycycline concentrations. Thus, self-communication, through a cell's small rate of basal secretion, primarily accounts for the "self-activation" at this low cell density (fig. S13). At a high total cell density (OD = 0.1), the sense-only strain's GFP signal increased at the same time and at the same rate as the secrete-and-sense cells, indicating that neighbor communication primarily caused the activation (fig. S13). Thus, at sufficiently high density, secrete-and-sense cells with positive feedback collectively amplify each cell's basal secretion of α-factor, leading to a "neighbor activation."

To summarize, self-activation can occur without any neighbor communication, whereas neighbor activation can occur in regimes where self-communication is insufficient for self-activation of the secrete-and-sense cells with the positive feedback link. Neighbor communication strengthens the positive feedback, enabling even a very weak positive feedback secrete-and-sense circuit to behave as if it had a strong positive feedback. Self-communication, through sufficiently strong positive feedback, enables the secrete-and-sense cells with a very low secretion rate to self-activate so that they can communicate with their neighbors. The interplay between self-communication and neighbor communication creates the overall population-level behavior, in which all cells activate in near unison (Fig. 3D) (*61*). Our work shows that understanding this collective behavior of the secrete-and-sense circuit with the positive feedback link requires knowing the properties of both the intracellular circuit and the communication between the secrete-and-sense cells.

### *Signal Degradation with Positive Feedback Enables Bimodal Cellular Differentiation*

We also examined the effects of an active signal degradation mechanism in secrete-and-sense circuits. We engineered our positive feedback–equipped basic secrete-and-sense strain to express the Bar1 protease (*50*, *52*–*54*), which degrades α-factor in the periplasmic space of the yeast cell (Fig. 4A). We constructed a set of such strains, each with a different constitutive promoter that controls the Bar1 expression (strength of promoters shown in figs. S8, S14, and S15).

A strain that had a weak constitutive expression level of Bar1 (Fig. 4, B and C, fig. S15) was incubated by itself at low (OD = 0.001) or high (OD = 0.1) cell density and in various concentrations of doxycycline. When its positive feedback was weak (for example, [doxycycline] = 6 μg/ml), the strain remained in the OFF state in the low cell density culture (Fig. 4B, left column) and was activated at high cell density (Fig. 4C, left column). Increasing expression of Bar1 decreased the rate at which activation occurred (fig. S15). When positive feedback was sufficiently strong (for example, [doxycycline] = 20 μg/ml), for the low (Fig. 4B, right column) and high (Fig. 4C, right column) cell densities, a transient mixture of OFF-state and ON-state cells was observed in the isogenic culture. In this bimodal population, consisting of isogenic cells that were all initially in the OFF state, all the cells in the OFF state were eventually activated to the ON state (fig. S15). At high cell density (OD = 0.1), the cells were activated faster (Fig. 4C, right column), consistent with our finding that increasing the degree of neighbor communication increased the rate at which the secrete-and-sense cells could be activated.

By examining the individual time courses for all our strains with Bar1 expression (fig. S14 and S15), we obtained a phase diagram that summarizes how the population-level behaviors depend on the positive feedback strength and the Bar1 abundance (Fig. 4D). From our mathematical model (*61*), we obtained an intuitive explanation of this phase diagram. When the cells express very high amounts of Bar1, no activation (self or neighbor) can occur because the high activity of Bar1 degrades the basally secreted α-factor produced by each cell. When the cell density is low, the secrete-and-sense cells rely on self-communication for their activation. If in the low cell density cultures, the secrete-and-sense cells

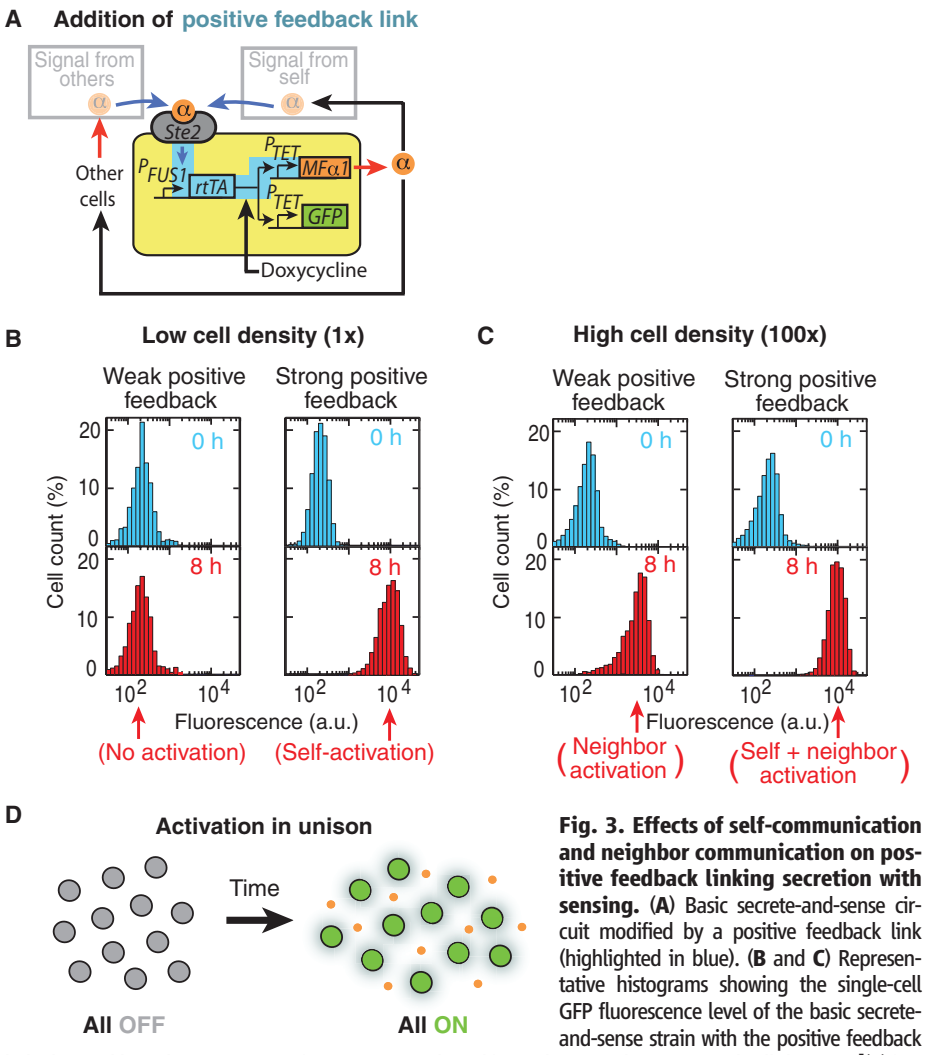


**Fig. 3. Effects of self-communication and neighbor communication on positive feedback linking secretion with sensing.** (**A**) Basic secrete-and-sense circuit modified by a positive feedback link (highlighted in blue). (**B** and **C**) Representative histograms showing the single-cell GFP fluorescence level of the basic secrete-and-sense strain with the positive feedback link obtained by a flow cytometer. This strain was cultured by itself at two different initial cell densities [(B) low cell density (OD = 0.001) and (C) high cell density (OD = 0.1)] and in two representative concentrations of doxycycline {[doxycycline] = 3 μg/ml (weak positive feedback) and 40 μg/ml (strong positive feedback)}. Blue histograms, beginning of the time course (0 hour); red histograms, 8 hours into the time course (full data sets in figs. S11 and S12). Under each panel, the corresponding type of activation behavior is mentioned. a.u., arbitrary units. (**D**) Main population-level behavior: activation of all cells in near unison.

express a low amount of Bar1 and use a strong positive feedback link, then they can self-activate in a digital (ON or OFF) manner, which manifests as a transient bimodal population of quiescent and maximally secreting cells (Fig. 4E). This results from cell-to-cell variability in the threshold for activation (that is, the amount of α-factor required for activation). At a sufficiently high cell density, neighbor activation dominates, and because every cell essentially senses the same concentrations of α-factors produced by collective basal secretion, the bimodal activation can disappear (as cell-to-cell variability becomes less relevant) and cells can activate together in a graded fashion (*61*). Without the positive feedback, signal degradation's role is weakening the secreted signal. However, when coupled with positive feedback, signal degradation has important effects on the population-level behaviors of secrete-and-sense circuits that reach beyond just weakening of the secreted signal. This may suggest why signal degradation mechanisms are often present in conjunction with positive feedback links in naturally occurring secrete-and-sense circuits. Bar1, coupled with positive feedback, enables a secrete-and-sense cell to delay its response to signal and a population to "hedge its bets" by responding in two distinct ways (that is, bimodal activation, Fig. 4E) by tuning the threshold for activation. Moreover, cells can suppress self-activation while only allowing neighbor activation.

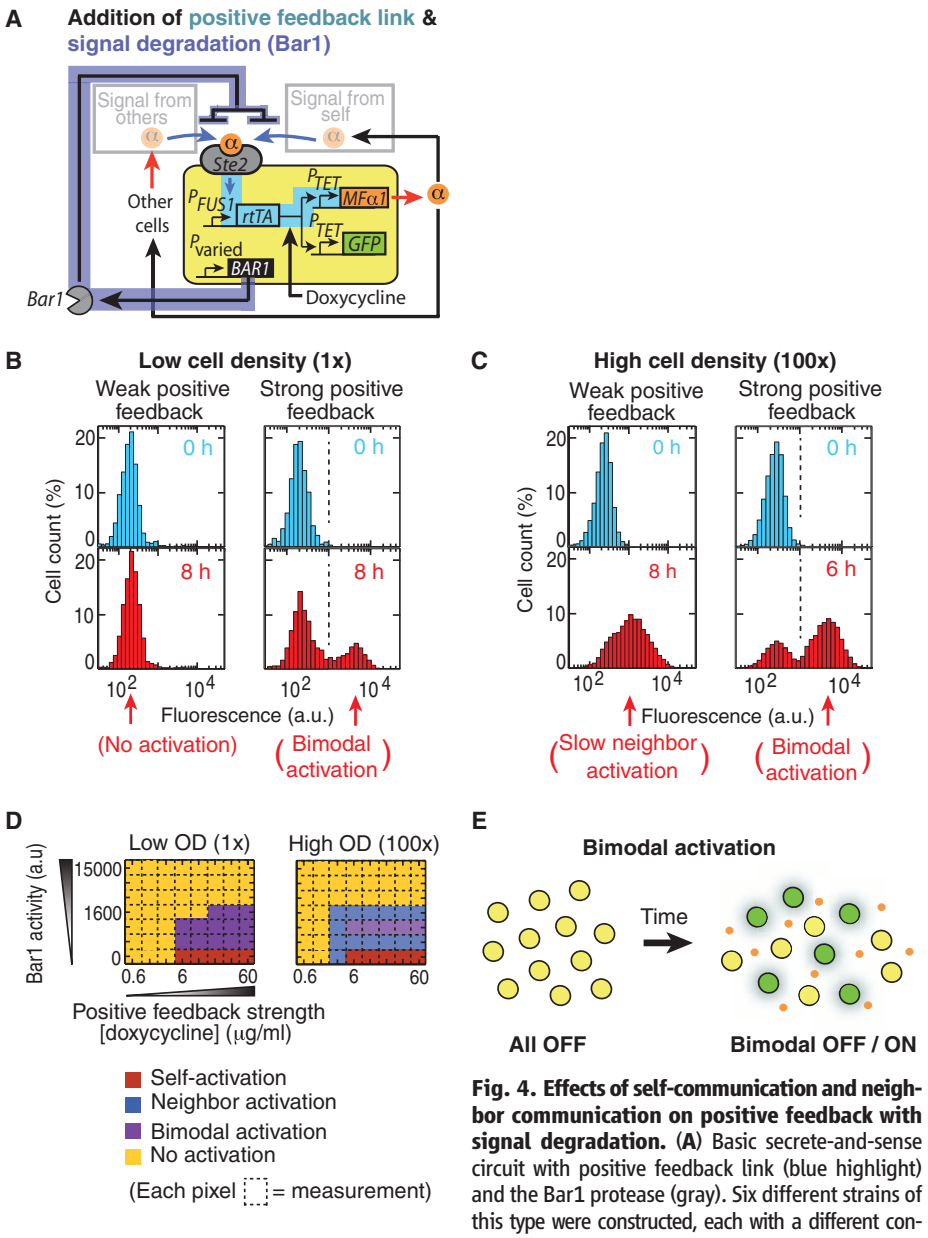


**Fig. 4. Effects of self-communication and neighbor communication on positive feedback with signal degradation.** (**A**) Basic secrete-and-sense circuit with positive feedback link (blue highlight) and the Bar1 protease (gray). Six different strains of this type were constructed, each with a different constitutive promoter $P_{varied}$ controlling expression of *BAR1*. (**B** and **C**) An example strain (with *pCYC1-BAR1*) cultured by itself at two different initial cell densities [(E) low cell density (OD = 0.001) and (F) high cell density (OD = 0.1)] and in two representative doxycycline concentrations {[doxycycline] = 6 μg/ml (weak positive feedback) and 20 μg/ml (strong positive feedback)}. Representative histograms showing the single-cell GFP fluorescence levels of this strain are plotted at two different time points (blue and red histograms). Under each panel, the corresponding type of activation behavior is mentioned (figs. S14 and S15). (**D**) Phase diagrams from analyzing each time course for the seven secrete-and-sense strains, each with different amounts of Bar1 (including none, Fig. 3) and positive feedback strengths at low (OD = 0.001) and high (OD = 0.1) cell density cultures (summarizes fig. S11, S12, S14, and S15). (**E**) Main population-level behavior: bifurcation of an isogenic population into subpopulations of transiently quiescent and maximally secreting cells.

### *Intuitive Phenomenological Model*

We developed a simple mathematical model that ties together various roles of self-communication and neighbor communication (*61*). Its central idea is that self-communication competes with neighbor communication because they both use the same molecule and receptor. A secrete-and-sense cell can build a locally high concentration of α-factor that it secreted. In low cell densities, this occurs faster than the rate at which the concentration far from the secrete-and-sense cell (the "global concentration") changes. Sensing of the locally high α-factor concentration leads to the fast increases in the secrete-and-sense cell's response (self-communication in Fig. 5A and fig. S16), whereas the slowly changing global concentration of the α-factor leads to a slow response in sense-only cells at low cell density (neighbor communication in Fig. 5A and figs. S17 to S19) (*61*). Paradoxically, self-communication in effect insulates a secrete-and-sense cell from responding to the α-factor that is secreted by the other secrete-and-sense cells. Our model quantifies and summarizes the degree of self-communication and neighbor communication in a phase diagram of these key features (Fig. 5B) (*61*). It also aids in understanding the competition between the positive feedback and the effects of the active signal degradation (figs. S20 to S23) (*61*). Our simple model thus provides an intuitive explanation of the main principles underlying the results of our experiments.

## Discussion

### *Translating Knowledge from Synthetic to Natural Systems*

By integrating simple mathematical models, measurements on single cells and whole populations, and a bottom-up synthetic biology approach, we revealed a diverse repertoire of biological functions that secrete-and-sense cells can achieve. Crucially, this integrated approach uncovered design principles that enable the circuit to tune the balance between self-communication and neighbor communication among cells—a crucial mechanism for achieving myriad cellular behaviors and an important general issue in biology. Our work provides a framework for designing synthetic secrete-and-sense circuits and better understanding of the diverse behaviors of seemingly disparate natural secrete-and-sense cells (Table 1). For example, bacterial quorum sensing—a purely social behavior (Fig. 5C)—relies on the low

secretion rate of an autoinducer and the low expression level of a low-affinity receptor to prohibit self-communication and allow only neighbor communication (*27*, *31*, *33*, *69*). Epithelial cells predominantly self-communicate through a signaling loop, commonly referred to as "autocrine signaling loop" (*38*–*49*, *70*–*74*), by expressing large amount of epidermal growth factor (EGF) receptor and secreting EGF, which the receptor recognizes, at sufficiently high rates (*73*)—a purely asocial behavior (Fig. 5C).

Self-activation (Fig. 5C) occurs in T helper ($T_H$) cells when they use positive feedback on the cytokine IL-2 that they secrete and sense to sharply increase their proliferation rate in a switch-like fashion. Specifically, $T_H$ cells increase both the expression of high-affinity IL-2 receptor and secretion rate of IL-2, which enhances their self-communication through IL-2 that enables them to turn on their proliferation switch. This promotes a monoclonal expansion of cells within an initially polyclonal population of T cells, even though all cells in the population have the same underlying network for processing IL-2 signal (*45*–*48*, *62*).

Aside from known cellular behaviors, our work suggests that simultaneous self-communication and neighbor communication may be a crucial mechanism to consider for interpreting behaviors of secrete-and-sense cells that are currently poorly understood. In particular, there are numerous examples of poorly understood cytokine-mediated decisions in immunology and developmental biology. For example, recent studies have revealed that naïve $T_H$ cells can realize a tunable hybrid of the two $T_H$ cell states, $T_H1$ and $T_H2$, which is controlled by secreting and sensing cytokines interferon-γ and IL-4 (*75*, *76*). Self-communication and neighbor communication through these cytokines have both been implicated as the main factors that determine the distribution of the hybrid cell fates in the population, but the details are unknown. Our work suggests that the simultaneous self-communication and neighbor communication in these T cells may be understood by measuring the cell density and individual T cell's receptor expression and secretion rate through single-cell measurement techniques. In the cells of developing embryos, secreting and sensing hedgehog signaling molecules such as the Sonic hedgehog (Shh) are crucial for cell fate specification, including in the embryos of fruit flies, mice, and humans (*77*). Although it is known that these cells use combinations of autocrine

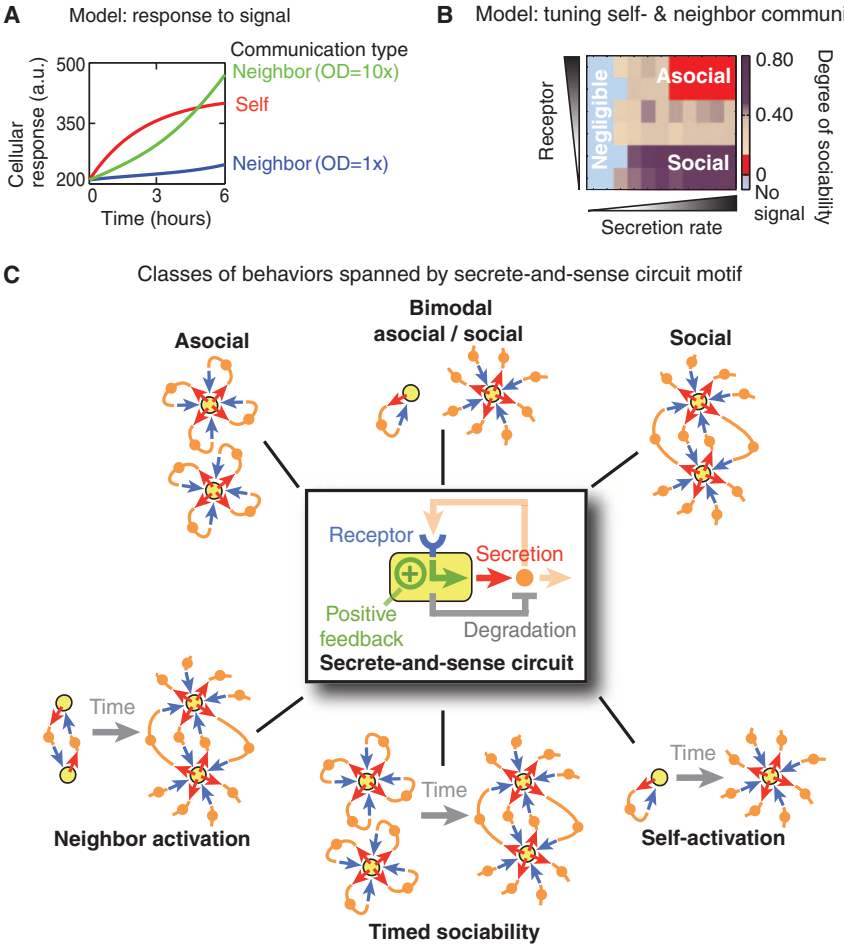


**Fig. 5. A simple mathematical model provides intuition.** (**A** and **B**) A phenomenological model provides qualitative insights underlying the main features of the secrete-and-sense circuit revealed by our experiments (*61*). (A) Model explains the individual cellular response of a secrete-and-sense cell that self-communicates (red curve) and of a sense-only cell at a low cell density (blue curve) and at a higher cell density (green curve). These curves are analogous to those seen in Fig. 2, C and D. (B) Model summarizes self-communication and neighbor communication in a phase diagram representing the "degree of sociability" [defined in the supplementary text (*61*)]. (**C**) Summary of the main behavioral classes spanned by the secrete-and-sense circuit motif.

**Table 1. Design table for engineering secrete-and-sense cells with desired biological functions motivated by our synthetic secrete-and-sense circuit.** Examples of biological functions of secrete-and-sense cells that can be understood and engineered on the basis of the design principles revealed by our synthetic circuit.

| Desired biological function | Possible circuit parameters for realizing desired biological function | Mode of communication used (neighbor/self) | Class of behavior (Fig. 5C) |
|---|---|---|---|
| Quorum sensing | Low receptor abundance<br>Weak positive feedback | Neighbor | Purely social |
| Monoclonal expansion of cells in a polyclonal culture due to sensing of self-secreted cytokines | High receptor abundance and high secretion rate<br>Strong positive feedback | Self | Purely asocial<br>Self-activation<br>Timed activation |
| Creating two functionally distinct cell states | Moderate to strong positive feedback | Self and neighbor | Self-activation<br>Neighbor activation<br>Timed activation |
| Differentiating an isogenic population into two populations of functionally distinct cells that coexist with a defined ratio | Moderate positive feedback with low signal degradation<br>Strong positive feedback with moderate signal degradation | Self and neighbor | Bimodal activation<br>Self-activation<br>Neighbor activation<br>Timed activation |

and paracrine signaling of hedgehog signaling molecules for proper cell fate specification, the difference in the dynamics of individual cells' response to the same signaling molecule determined by self-communication and neighbor communication has not received much attention. Insights provided by recent studies on quantitative single-cell dynamics in developing embryos indicate that the different time scales of individual cell's response, such as those that would be generated by self-communication and neighbor communication through the same molecule, are central for a reliable and timely developmental patterning that is reproducible between individuals (*78*–*83*). This is especially true in spatially organized cells—an important scenario that our work did not address. Our work suggests that in addition to identifying the signaling pathways, the approaches we use to distinguish whether a pathway is self- or neighbor-activated is crucial to understand the developmental process of animals.

In engineering secrete-and-sense cells, our work shows that it is possible to design microbes that can achieve "diffusion sensing" (*84*), a hypothetical mechanism for self-communication in bacteria akin to mammalian autocrine signaling (*70*), which was proposed but lacked a clear demonstration. Our work suggests that by increasing the receptor expression of bacteria that sense a quorum, they can be converted to diffuse sense, which may be useful in bioproduction applications. Such cells may integrate self-sensing and quorum sensing to make sophisticated and autonomous decisions about optimal switching times between growth and production phases. Indeed, some of the yeast strains engineered in our study may be useful for large-scale biofermentation, in which adding external inducer molecules is prohibitively expensive. Moreover, the ability to tune self-communication versus neighbor communication in multicellular microbial systems, such as the social amoebae *Dictyostelium discoideum* or biofilms, may provide a way to better understand the advantages of cooperative versus self-driven behaviors (*20*–*25*, *85*, *86*).

Evolution appears to favor efficient circuits and signaling elements that can accomplish many different tasks (*13*, *14*). The diverse social behaviors that are enabled by the functional flexibility of the secrete-and-sense circuits (Fig. 5C) may explain the frequent occurrence of this class of circuits in nature.

### *Dissecting Multicellular Behaviors Through Bottom-Up Synthetic Biology Approach*

Beyond understanding secrete-and-sense circuits, our approach may be generalized to reveal how cells use fundamental cell signaling circuits to achieve complex multicellular behaviors. Synthetic cell signaling circuits, including some capable of quorum sensing, have often been used to demonstrate targeted cellular behaviors and engineering goals (for example, cellular logic gates) (*3*, *28*, *33*, *34*, *37*, *87*–*94*). Our work highlights the alternate use of synthetic circuits—for exploring their full capabilities and understanding them in a framework that unites natural and synthetic multicellular systems that share the same circuit motif (*95*–*97*). Although only a handful of canonical signaling pathways and circuit motifs are repeatedly used across species, how they produce multicellular behaviors is poorly understood at a systems level (*98*). By building synthetic signaling circuits that mimic the natural signaling circuits, one can perturb each circuit element in individual cells, measure its effects on intracellular and intercellular interactions, and then bridge these interactions to the whole population-level behavior. Doing so may help us understand how the myriad interactions from molecules to cells are coordinated to yield coherent, higher-order macroscopic multicellular behaviors (*2*).

## Materials and Methods

### *Plasmid and Strain Construction*

A list of yeast strains used in our study is in table S1, and a list of single-copy yeast-integrating plasmids is in table S2. Full details of plasmid and strain construction are available in the materials and methods. Here, we summarize the yeast and plasmid constructs and the basic construction process. All strains were derived from the haploid strain W303 (*MATa his3 trp1 leu2 ura3*). In particular, the strains CB008 and CB009 (table S1) (*51*), which were both derived from W303 and *far1*Δ, were our starting base strains for generating all other strains. The family tree of our strains and their genotypes are provided in table S1. Two main differences between CB008 and CB009 are that CB008 contains the endogenous BAR1 and lacks pFUS1-GFP, whereas CB009 is *bar1*Δ and has pFUS1-GFP integrated at the mfa2 locus. We knocked out genes in yeast using the standard polymerase chain reaction (PCR)–mediated gene deletion method, in which the undesired gene in the yeast genome is swapped with a PCR product that contains the selective marker gene in its place through a homologous recombination. The selection markers we used were as follows: *HIS3*, *URA3*, *TRP1*, *LEU2*, *KanMX* (resistance to G418, Geneticin, Life Technologies), *HphMX* (resistance to hygromycin B, Life Technologies), and *natMX* (resistance to nourseothricin, Sigma-Aldrich). Yeast transformations were performed with the standard polyethylene glycol/lithium acetate method.

### *Flow Cytometry*

Single-cell fluorescence was measured using a Becton Dickinson LSRII (custom-designed) flow cytometer with a robotic arm for handling samples in a 96-well plate. GFP fluorescence was measured using a coherent sapphire laser with an excitation wavelength of 488 nm. For both dose response and time course experiments, unless otherwise stated, sample aliquots were treated with cycloheximide (5 μg/ml) (Sigma-Aldrich) before measuring single-cell fluorescence. In obtaining the single-cell mean fluorescence values, differences in cell sizes were accounted for through forward and side scatter distributions in the flow cytometer, thus ensuring fair comparisons of fluorescence values.

### *Culturing Yeast Strains*

We cultured all our yeast strains in a standard synthetic medium with 2% glucose at 30°C. For inducing gene expression in yeast with doxycycline ("doxycycline hyclate, 98% purity," Sigma-Aldrich), we aliquoted previously dissolved doxycycline (in double-distilled water) directly into the growth medium to a desired final concentration. Unless otherwise stated, all our yeast strains were cultured in 5 ml of synthetic medium that was constantly mixed by a rotatory wheel at 30°C. For induction with α-factor (Zymo Research), cells were cultured with desired amounts of the α-factor in 5 ml of synthetic medium.

### *Main Features of Mathematical Model*

Full details of our mathematical model and step-by-step derivations of all the equations listed below are available in the supplementary text. Here, we summarize basic mathematical techniques and physical intuition used in building our model. The main physics underlying our model is the notion of "mixing length scale" from fluid mechanics (*99*). It characterizes the distance over which a fluid element (coherent collection of fluid molecules) can travel before losing its collective properties and mixing with the rest of the fluid. A fluid element smoothly flows in the laminar flow region, but upon crossing the boundary between laminar and turbulent flow regimes, its collective motion is destroyed as its individual fluid molecules mix with the surrounding fluid (*99*). When a mechanical device is rotating a tube that contains a liquid medium, such as in our experiments, the device cannot transmit its energy efficiently down to an arbitrarily small length scale to break off all fluid elements. As detailed in our calculations in the supplementary text, this led to a turbulent flow in the macroscopic length scale (on the order of millimeters) but a laminar flow in the microscopic length scales (below about 500 μm, depending on the Reynolds number) in our experimental setup. Hence, a secrete-and-sense cell could create and maintain a concentration gradient of α-factor around itself in our cultures. As shown in the supplementary text, at OD = 0.1 and a high Reynolds number of 10,000, we computed the Kolmogorov mixing length scale (*99*) for our experimental setup to be about 30 μm, which was about five times larger than the average diameter of haploid yeast cells (*61*). A more realistic lower Reynolds number yielded a larger Kolmogorov mixing length. Hence, a secrete-and-sense cell could self-communicate by sensing the concentration gradient formed by the α-factor that it secreted, which could be maintained just around the cell and determined by solving the diffusion equation. Beyond a distance from the cell that is larger than the Kolmogorov mixing length, α-factor from all secrete-and-sense cells became "well mixed" together because of the turbulent flow regime. For this regime, we used a "mean field" approximation to compute the α-factor concentration. As detailed

in the supplementary text, solving the diffusion equation in three dimensions with the appropriate boundary conditions (constant secretion rate, no α-factor infinitely far away from the cell) yielded the concentration $c$ over time $t$ of α-factor at the surface of the secrete-and-sense cell with radius $R$ (*100*) (also eq. S1 in the supplementary text):

$$c(R,t) = \frac{\sqrt{t}F_0}{\sqrt{\pi}D}\left\{1 - e^{\frac{-R^2}{Dt}} + \frac{R\sqrt{\pi}}{\sqrt{Dt}}erfc\left(\frac{R}{\sqrt{Dt}}\right)\right\} \quad (1)$$

where $D$ is the diffusion coefficient of α-factor in water [$D$ = 150 $\mu m^2/s$, estimated by using the Stokes-Einstein relation and is similar to the value used by more detailed and insightful models of the mating pathway (*53*, *54*)] and $F_0$ is the flux of the α-factor molecules secreted radially outward at the cell surface [molecules/(area × time)]. From Eq. 1, we used the standard first-order ordinary differential equation model for constitutive gene expression to derive the basic secrete-and-sense cell's GFP abundance $G_{self}$ due to pure self-communication, which was described by Eq. 2 (also eq. S3 in the supplementary text):

$$G_{self}([\alpha],t) = \left(G_0 - \frac{k([\alpha])}{\sigma}\right)e^{-\sigma t} + \frac{k([\alpha])}{\sigma} \quad (2)$$

where $G_0$ is the basal GFP level, σ is the first-order protein degradation rate of GFP, and $k([\alpha])$ is the net production rate (transcription and translation combined) of GFP as a function of the concentration of α-factor. Specific values for these parameters were determined as detailed in the supplementary text (*61*). We used a similar approach to model neighbor communication, resulting in Eq. 3 that described the basic sense-only cell's GFP level $G_{others}$ (also see eq. S6 in the supplementary text):

$$\frac{dG_{others}}{dt} = k(\rho(t)) - \sigma G_{others} \quad (3)$$

where $\rho(t)$ is the global concentration of the α-factor due to the collective secretion of all the secrete-and-sense cells (details in the supplementary text). By numerically solving Eq. 3, we obtained $G_{others}$. Equations 2 and 3 together quantified the degrees of self-communication and neighbor communication in our secrete-and-sense cells. Full details of these analyses are available in the supplementary text.

### References and Notes


1. Y. Afek *et al.*, A biological solution to a fundamental distributed computing problem. *Science* **331**, 183–185 (2011). doi: 10.1126/science.1193210; pmid: 21233379
2. P. Mehta, T. Gregor, Approaching the molecular origins of collective dynamics in oscillating cell populations. *Curr. Opin. Genet. Dev.* **20**, 574–580 (2010). doi: 10.1016/j.gde.2010.09.004; pmid: 20934869
3. O. Mondragón-Palomino, T. Danino, J. Selimkhanov, L. Tsimring, J. Hasty, Entrainment of a population of synthetic genetic oscillators. *Science* **333**, 1315–1319 (2011). doi: 10.1126/science.1205369; pmid: 21885786
4. D. Sprinzak *et al.*, *Cis*-interactions between Notch and Delta generate mutually exclusive signalling states. *Nature* **465**, 86–90 (2010). doi: 10.1038/nature08959; pmid: 20418862
5. G. von Dassow, E. Meir, E. M. Munro, G. M. Odell, The segment polarity network is a robust developmental module. *Nature* **406**, 188–192 (2000). doi: 10.1038/35018085; pmid: 10910359
6. J. V. Wong, B. Li, L. You, Tension and robustness in multitasking cellular networks. *PLOS Comput. Biol.* **8**, e1002491 (2012). doi: 10.1371/journal.pcbi.1002491; pmid: 22577355
7. W. H. de Ronde, F. Tostevin, P. R. ten Wolde, Multiplexing biochemical signals. *Phys. Rev. Lett.* **107**, 048101 (2011). doi: 10.1103/PhysRevLett.107.048101; pmid: 21867046
8. R. Hermsen, B. Ursem, P. R. ten Wolde, Combinatorial gene regulation using auto-regulation. *PLOS Comput. Biol.* **6**, e1000813 (2010). doi: 10.1371/journal.pcbi.1000813; pmid: 20548950
9. J. Y. Chen, J. R. Lin, K. A. Cimprich, T. Meyer, A two-dimensional ERK-AKT signaling code for an NGF-triggered cell-fate decision. *Mol. Cell* **45**, 196–209 (2012). doi: 10.1016/j.molcel.2011.11.023; pmid: 22206868
10. T. Bollenbach, R. Kishony, Resolution of gene regulatory conflicts caused by combinations of antibiotics. *Mol. Cell* **42**, 413–425 (2011). doi: 10.1016/j.molcel.2011.04.016; pmid: 21596308
11. L. Espinar, M. Dies, T. Cagatay, G. M. Süel, J. Garcia-Ojalvo, Circuit-level input integration in bacterial gene regulation. *Proc. Natl. Acad. Sci. U.S.A.* **110**, 7091–7096 (2013). doi: 10.1073/pnas.1216091110; pmid: 23572583
12. Y. Hart, U. Alon, The utility of paradoxical components in biological circuits. *Mol. Cell* **49**, 213–221 (2013). doi: 10.1016/j.molcel.2013.01.004; pmid: 23352242
13. S. S. Shen-Orr, R. Milo, S. Mangan, U. Alon, Network motifs in the transcriptional regulation network of *Escherichia coli*. *Nat. Genet.* **31**, 64–68 (2002). doi: 10.1038/ng881; pmid: 11967538
14. R. Milo *et al.*, Network motifs: Simple building blocks of complex networks. *Science* **298**, 824–827 (2002). doi: 10.1126/science.298.5594.824; pmid: 12399590
15. J. Gao, S. V. Buldyrev, H. E. Stanley, S. Havlin, Networks formed from interdependent networks. *Nat. Phys.* **8**, 40–48 (2012). doi: 10.1038/nphys2180
16. E. H. Davidson, Emerging properties of animal gene regulatory networks. *Nature* **468**, 911–920 (2010). doi: 10.1038/nature09645; pmid: 21164479
17. J. E. Purvis, G. Lahav, Encoding and decoding cellular information through signaling dynamics. *Cell* **152**, 945–956 (2013). doi: 10.1016/j.cell.2013.02.005; pmid: 23452846
18. J. Tegner, M. K. S. Yeung, J. Hasty, J. J. Collins, Reverse engineering gene networks: Integrating genetic perturbations with dynamical modeling. *Proc. Natl. Acad. Sci. U.S.A.* **100**, 5944–5949 (2003). doi: 10.1073/pnas.0933416100; pmid: 12730377
19. J. E. Ferrell Jr. *et al.*, Simple, realistic models of complex biological processes: Positive feedback and bistability in a cell fate switch and a cell cycle oscillator. *FEBS Lett.* **583**, 3999–4005 (2009). doi: 10.1016/j.febslet.2009.10.068; pmid: 19878681
20. T. Gregor, K. Fujimoto, N. Masaki, S. Sawai, The onset of collective behavior in social amoebae. *Science* **328**, 1021–1025 (2010). doi: 10.1126/science.1183415; pmid: 20413456
21. S. De Monte, F. d'Ovidio, S. Danø, P. Graae Sørensen, Dynamical quorum sensing: Population density encoded in cellular dynamics. *Proc. Natl. Acad. Sci. U.S.A.* **104**, 18377–18381 (2007). doi: 10.1073/pnas.0706089104; pmid: 18003917
22. D. J. Schwab, A. Baetica, P. Mehta, Dynamical quorum-sensing in oscillators coupled through an external medium. *Physica D* **241**, 1782–1788 (2012). doi: 10.1016/j.physd.2012.08.005; pmid: 23087494
23. S. Sawai, P. A. Thomason, E. C. Cox, An autoregulatory circuit for long-range self-organization in *Dictyostelium* cell populations. *Nature* **433**, 323–326 (2005). doi: 10.1038/nature03228; pmid: 15662425
24. L. Li, E. C. Cox, H. Flyvbjerg, 'Dicty dynamics': Dictyostelium motility as persistent random motion. *Phys. Biol.* **8**, 046006 (2011). doi: 10.1088/1478-3975/8/4/046006; pmid: 21610290
25. T. Umeda, K. Inouye, Cell sorting by differential cell motility: A model for pattern formation in Dictyostelium. *J. Theor. Biol.* **226**, 215–224 (2004). doi: 10.1016/j.jtbi.2003.08.016; pmid: 14643191
26. W. L. Ng, B. L. Bassler, Bacterial quorum-sensing network architectures. *Annu. Rev. Genet.* **43**, 197–222 (2009). doi: 10.1146/annurev-genet-102108-134304; pmid: 19686078
27. K. C. Tu, T. Long, S. L. Svenningsen, N. S. Wingreen, B. L. Bassler, Negative feedback loops involving small regulatory RNAs precisely control the *Vibrio harveyi* quorum-sensing response. *Mol. Cell* **37**, 567–579 (2010). doi: 10.1016/j.molcel.2010.01.022; pmid: 20188674
28. L. You, R. S. Cox III, R. Weiss, F. H. Arnold, Programmed population control by cell-cell communication and regulated killing. *Nature* **428**, 868–871 (2004). doi: 10.1038/nature02491; pmid: 15064770
29. I. B. Bischofs, J. A. Hug, A. W. Liu, D. M. Wolf, A. P. Arkin, Complexity in bacterial cell–cell communication: Quorum signal integration and subpopulation signaling in the *Bacillus subtilis* phosphorelay. *Proc. Natl. Acad. Sci. U.S.A.* **106**, 6459–6464 (2009). doi: 10.1073/pnas.0810878106; pmid: 19380751
30. P. Mehta, S. Goyal, T. Long, B. L. Bassler, N. S. Wingreen, Information processing and signal integration in bacteria quorum sensing. *Mol. Syst. Biol.* **5**, 325 (2009). doi: 10.1038/msb.2009.79; pmid: 19920810
31. A. Eldar, Social conflict drives the evolutionary divergence of quorum sensing. *Proc. Natl. Acad. Sci. U.S.A.* **108**, 13635–13640 (2011). doi: 10.1073/pnas.1102923108; pmid: 21807995
32. A. Pai, Y. Tanouchi, L. You, Optimality and robustness in quorum sensing (QS)-mediated regulation of a costly public good enzyme. *Proc. Natl. Acad. Sci. U.S.A.* **109**, 19810–19815 (2012). doi: 10.1073/pnas.1211072109; pmid: 23144221
33. T. C. Williams, L. K. Nielsen, C. E. Vickers, Engineered quorum sensing using pheromone-mediated cell-to-cell communication in *Saccharomyces cerevisiae*. *ACS Synth. Biol.* **2**, 136–149 ( 2013). doi: 10.1021/sb300110b; pmid: 23656437
34. T. Danino, O. Mondragón-Palomino, L. Tsimring, J. Hasty, A synchronized quorum of genetic clocks. *Nature* **463**, 326–330 (2010). doi: 10.1038/nature08753; pmid: 20090747
35. S. W. Teng *et al.*, Active regulation of receptor ratios controls integration of quorum-sensing signals in *Vibrio harveyi*. *Mol. Syst. Biol.* **7**, 491 (2011). doi: 10.1038/msb.2011.30; pmid: 21613980
36. A. Chatterjee *et al.*, Antagonistic self-sensing and mate-sensing signaling controls antibiotic-resistance transfer. *Proc. Natl. Acad. Sci. U.S.A.* **110**, 7086–7090 (2013). doi: 10.1073/pnas.1212256110; pmid: 23569272
37. M. T. Chen, R. Weiss, Artificial cell-cell communication in yeast *Saccharomyces cerevisiae* using signaling elements from *Arabidopsis thaliana*. *Nat. Biotechnol.* **23**, 1551–1555 (2005). doi: 10.1038/nbt1162; pmid: 16299520
38. I. B. Leibiger, B. Leibiger, P. O. Berggren, Insulin signaling in the pancreatic β-cell. *Annu. Rev. Nutr.* **28**, 233–251 (2008). doi: 10.1146/annurev.nutr.28.061807.155530; pmid: 18481923
39. C. A. Aspinwall, J. R. T. Lakey, R. T. Kennedy, Insulin-stimulated insulin secretion in single pancreatic beta cells. *J. Biol. Chem.* **274**, 6360–6365 (1999). doi: 10.1074/jbc.274.10.6360; pmid: 10037726
40. E. Hoyos *et al.*, Quantitative variation in autocrine signaling and pathway crosstalk in the *Caenorhabditis* vulval network. *Curr. Biol.* **21**, 527–538 (2011). doi: 10.1016/j.cub.2011.02.040; pmid: 21458263
41. N. Chen, I. Greenwald, The lateral signal for LIN-12/Notch in *C. elegans* vulval development comprises redundant secreted and transmembrane DSL proteins. *Dev. Cell* **6**, 183–192 (2004). doi: 10.1016/S1534-5807(04)00021-8; pmid: 14960273
42. G. Seydoux, I. Greenwald, Cell autonomy of *lin-12* function in a cell fate decision in *C. elegans*. *Cell* **57**, 1237–1245 (1989). doi: 10.1016/0092-8674(89)90060-3; pmid: 2736627
43. P. W. Sternberg, H. R. Horvitz, The combined action of two intercellular signaling pathways specifies three cell fates during vulval induction in *C. elegans*. *Cell* **58**, 679–693 (1989). doi: 10.1016/0092-8674(89)90103-7; pmid: 2548732

44. F. Corson, E. D. Siggia, Geometry, epistasis, and developmental patterning. *Proc. Natl. Acad. Sci. U.S.A.* **109**, 5568–5575 (2012). doi: 10.1073/pnas.1201505109; pmid: 22434912
45. D. A. Cantrell, K. A. Smith, The interleukin-2 T-cell system: A new cell growth model. *Science* **224**, 312–1316 (1984). doi: 10.1126/science.6427923; pmid: 6427923
46. T. A. Waldmann, The biology of interleukin-2 and interleukin-15: Implications for cancer therapy and vaccine design. *Nat. Rev. Immunol.* **6**, 595–601 (2006). doi: 10.1038/nri1901; pmid: 16868550
47. Y. Savir, N. Waysbort, Y. E. Antebi, T. Tlusty, N. Friedman, Balancing speed and accuracy of polyclonal T cell activation: A role for extracellular feedback. *BMC Syst. Biol.* **6**, 111 (2012). doi: 10.1186/1752-0509-6-111; pmid: 22925037
48. O. Feinerman *et al*., Single-cell quantification of IL-2 response by effector and regulatory T cells reveals critical plasticity in immune response. *Mol. Syst. Biol.* **6**, 437 (2010). doi: 10.1038/msb.2010.90; pmid: 21119631
49. E. M. Fallon, D. A. Lauffenburger, Computational model for effects of ligand/receptor binding properties on interleukin-2 trafficking dynamics and T cell proliferation response. *Biotechnol. Prog.* **16**, 905–916 (2000). doi: 10.1021/bp000097t; pmid: 11027188
50. L. Bardwell, A walk-through of the yeast mating pheromone response pathway. *Peptides* **25**, 1465–1476 (2004). doi: 10.1016/j.peptides.2003.10.022;pmid: 15374648
51. C. J. Bashor, N. C. Helman, S. Yan, W. A. Lim, Using engineered scaffold interactions to reshape MAP kinase pathway signaling dynamics. *Science* **319**, 1539–1543 (2008). doi: 10.1126/science.1151153; pmid: 18339942
52. N. Barkai, M. Rose, N. Wingreen, Protease helps yeast find mating partners. *Nature* **396**, 422–423 (1998). doi: 10.1038/24760; pmid: 9853747
53. N. Rappaport, N. Barkai, Disentangling signaling gradients generated by equivalent sources. *J. Biol. Phys.* **38**, 267–278 (2012). doi: 10.1007/s10867-011-9240-x; pmid: 23450187
54. M. Jin *et al*., Yeast dynamically modify their environment to achieve better mating efficiency. *Sci. Signal.* **4**, ra54 (2011). doi: 10.1126/scisignal.2001763; pmid: 21868361
55. J. Gonçalves-Sá, A. Murray, Asymmetry in sexual pheromones is not required for ascomycete mating. *Curr. Biol.* **21**, 1337–1346 (2011). doi: 10.1016/j.cub.2011.06.054; pmid: 21835624
56. N. Hao *et al*., Regulation of cell signaling dynamics by the protein kinase-scaffold Ste5. *Mol. Cell* **30**, 649–656 (2008). doi: 10.1016/j.molcel.2008.04.016; pmid: 18538663
57. N. T. Ingolia, A. W. Murray, Positive-feedback loops as a flexible biological module. *Curr. Biol.* **17**, 668–677 (2007). doi: 10.1016/j.cub.2007.03.016; pmid: 17398098
58. R. C. Yu *et al*., Negative feedback that improves information transmission in yeast signalling. *Nature* **456**, 755–761 (2008). doi: 10.1038/nature07513; pmid: 19079053
59. H. D. Madhani, *From a to α: Yeast as a Model for Cellular Differentiation* (Cold Spring Harbor Laboratory Press, New York, 2006).
60. E. McCullagh, A. Seshan, H. El-Samad, H. D. Madhani, Coordinate control of gene expression noise and interchromosomal interactions in a MAP kinase pathway. *Nat. Cell Biol.* **12**, 954–962 (2010). doi: 10.1038/ncb2097; pmid: 20852627
61. Full details are available as supplementary materials on *Science* Online.
62. Y. Hart, Y. E. Antebi, A. E. Mayo, N. Friedman, U. Alon, Design principles of cell circuits with paradoxical components. *Proc. Natl. Acad. Sci. U.S.A.* **109**, 8346–8351 (2012). doi: 10.1073/pnas.1117475109; pmid: 22562798
63. J. E. Ferrell Jr., Feedback regulation of opposing enzymes generates robust, all-or-none bistable responses. *Curr. Biol.* **18**, R244–R245 (2008). doi: 10.1016/j.cub.2008.02.035; pmid: 18364225
64. G. Hornung, N. Barkai, Noise propagation and signaling sensitivity in biological networks: A role for positive feedback. *PLOS Comp. Biol.* **4**, e8 (2008). doi: 10.1371/journal.pcbi.0040008; pmid: 18179281
65. J. Hasty, J. Pradines, M. Dolnik, J. J. Collins, Noise-based switches and amplifiers for gene expression. *Proc. Natl. Acad. Sci. U.S.A.* **97**, 2075–2080 (2000). doi: 10.1073/pnas.040411297; pmid: 10681449
66. R. Hermsen, D. Erickson, T. Hwa, Speed, sensitivity, and bistability in auto-activating signaling circuits. *PLOS Comput. Biol.* **7**, e1002265 (2011). doi: 10.1371/journal.pcbi.1002265; pmid: 22125482
67. O. Feinerman, J. Veiga, J. R. Dorfman, R. N. Germain, G. Altan-Bonnet, Variability and robustness in T cell activation from regulated heterogeneity in protein levels. *Science* **321**, 1081–1084 (2008). doi: 10.1126/science.1158013; pmid: 18719282
68. P. Sansone *et al*., IL-6 triggers malignant features in mammospheres from human ductal breast carcinoma and normal mammary gland. *J. Clin. Invest.* **117**, 3988–4002 (2007). doi: 10.1172/JCI32533; pmid: 18060036
69. T. Long *et al*., Quantifying the integration of quorum-sensing signals with single-cell resolution. *PLOS Biol.* **7**, e68 (2009). doi: 10.1371/journal.pbio.1000068; pmid: 19320539
70. M. B. Sporn, G. J. Todaro, Autocrine secretion and malignant transformation of cells. *N. Engl. J. Med.* **303**, 878–880 (1980). doi: 10.1056/NEJM198010093031511; pmid: 7412807
71. M. Coppey, A. M. Berezhkovskii, S. C. Sealfon, S. Y. Shvartsman, Time and length scales of autocrine signals in three dimensions. *Biophys. J.* **93**, 1917–1922 (2007). doi: 10.1529/biophysj.107.109736; pmid: 17720734
72. S. Y. Shvartsman, H. S. Wiley, W. M. Deen, D. A. Lauffenburger, Spatial range of autocrine signaling: Modeling and computational analysis. *Biophys. J.* **81**, 1854–1867 (2001). doi: 10.1016/S0006-3495(01)75837-7; pmid: 11566760
73. A. E. DeWitt, J. Y. Dong, H. S. Wiley, D. A. Lauffenburger, Quantitative analysis of the EGF receptor autocrine system reveals cryptic regulation of cell response by ligand capture. *J. Cell Sci.* **114**, 2301–2313 (2001). pmid: 11493669
74. S. Y. Shvartsman *et al*., Autocrine loops with positive feedback enable context-dependent cell signaling. *Am. J. Physiol. Cell Physiol.* **282**, C545–C559 (2002). doi: 10.1152/ajpcell.00260.2001; pmid: 11832340
75. Y. E. Antebi *et al*., Mapping differentiation under mixed culture conditions reveals a tunable continuum of T cell fates. *PLOS Biol.* **11**, e1001616 (2013). doi: 10.1371/journal.pbio.1001616; pmid: 23935451
76. M. Fang, H. Xie, S. K. Dougan, H. Ploegh, A. van Oudenaarden, Stochastic cytokine expression induces mixed T helper cell states. *PLOS Biol.* **11**, e1001618 (2013). doi: 10.1371/journal.pbio.1001618; pmid: 23935453
77. L. Lum, P. A. Beachy, The Hedgehog response network: Sensors, switches, and routers. *Science* **304**, 1755–1759 (2004). doi: 10.1126/science.1098020; pmid: 15205520
78. T. Gregor, D. W. Tank, E. F. Wieschaus, W. Bialek, Probing the limits to positional information. *Cell* **130**, 153–164 (2007). doi: 10.1016/j.cell.2007.05.025; pmid: 17632062
79. F. Liu, A. H. Morrison, T. Gregor, Dynamic interpretation of maternal inputs by the Drosophila segmentation gene network. *Proc. Natl. Acad. Sci. U.S.A.* **110**, 6724–6729 (2013). doi: 10.1073/pnas.1220912110; pmid: 23580621
80. H. G. Garcia, M. Tikhonov, A. Lin, T. Gregor, Quantitative imaging of transcription in living Drosophila embryos links polymerase activity to patterning. *Curr. Biol.* **23**, 2140–2145 (2013). doi: 10.1016/j.cub.2013.08.054; pmid: 24139738
81. J. O. Dubuis, R. Samanta, T. Gregor, Accurate measurements of dynamics and reproducibility in small genetic networks. *Mol. Syst. Biol.* **9**, 639 (2013). doi: 10.1038/msb.2012.72; pmid: 23340845
82. M. Haskel-Ittah *et al*., Self-organized shuttling: Generating sharp dorsoventral polarity in the early *Drosophila* embryo. *Cell* **150**, 1016–1028 (2012). doi: 10.1016/j.cell.2012.06.044; pmid: 22939625
83. D. Ben-Zvi, B. Z. Shilo, A. Fainsod, N. Barkai, Scaling of the BMP activation gradient in *Xenopus* embryos. *Nature* **453**, 1205–1211 (2008). doi: 10.1038/nature07059; pmid: 18580943
84. R. J. Redfield, Is quorum sensing a side effect of diffusion sensing? *Trends Microbiol.* **10**, 365–370 (2002). doi: 10.1016/S0966-842X(02)02400-9; pmid: 12160634
85. D. A. Brock, T. E. Douglas, D. C. Queller, J. E. Strassmann, Primitive agriculture in a social amoeba. *Nature* **469**, 393–396 (2011). doi: 10.1038/nature09668; pmid: 21248849
86. J. Gore, H. Youk, A. van Oudenaarden, Snowdrift game dynamics and facultative cheating in yeast. *Nature* **459**, 253–256 (2009). doi: 10.1038/nature07921; pmid: 19349960
87. S. Basu, Y. Gerchman, C. H. Collins, F. H. Arnold, R. Weiss, A synthetic multicellular system for programmed pattern formation. *Nature* **434**, 1130–1134 (2005). doi: 10.1038/nature03461; pmid: 15858574
88. J. J. Tabor *et al*., A synthetic genetic edge detection program. *Cell* **137**, 1272–1281 (2009). doi: 10.1016/j.cell.2009.04.048; pmid: 19563759
89. F. K. Balagaddé *et al*., A synthetic *Escherichia coli* predator–prey ecosystem. *Mol. Syst. Biol.* **4**, 187 (2008). doi: 10.1038/msb.2008.24; pmid: 18414488
90. A. Tamsir, J. J. Tabor, C. A. Voigt, Robust multicellular computing using genetically encoded NOR gates and chemical 'wires'. *Nature* **469**, 212–215 (2011). doi: 10.1038/nature09565; pmid: 21150903
91. S. Regot *et al*., Distributed biological computation with multicellular engineered networks. *Nature* **469**, 207–211 (2011). doi: 10.1038/nature09679; pmid: 21150900
92. K. E. Galloway, E. Franco, C. D. Smolke, Dynamically reshaping signaling networks to program cell fate via genetic controllers. *Science* **341**, 1235005 (2013). doi: 10.1126/science.1235005; pmid: 23950497
93. J. Bonnet, P. Yin, M. E. Ortiz, P. Subsoontorn, D. Endy, Amplifying genetic logic gates. *Science* **340**, 599–603 (2013). doi: 10.1126/science.1232758; pmid: 23539178
94. C. Liu *et al*., Sequential establishment of stripe patterns in an expanding cell population. *Science* **334**, 238–241 (2011). doi: 10.1126/science.1209042; pmid: 21998392
95. M. B. Elowitz, W. A. Lim, Build life to understand it. *Nature* **468**, 889–890 (2010). doi: 10.1038/468889a; pmid: 21164460
96. A. Velenich, J. Gore, Synthetic approaches to understanding biological constraints. *Curr. Opin. Chem. Biol.* **16**, 323–328 (2012). doi: 10.1016/j.cbpa.2012.05.199; pmid: 22682889
97. S. Chen, P. Harrigan, B. Heineike, J. Stewart-Ornstein, H. El-Samad, Building robust functionality in synthetic circuits using engineered feedback regulation. *Curr. Opin. Biotechnol.* **24**, 790–796 (2013). doi: 10.1016/j.copbio.2013.02.025; pmid: 23566378
98. N. Perrimon, N. Barkai, The era of systems developmental biology. *Curr. Opin. Genet. Dev.* **21**, 681–683 (2011). doi: 10.1016/j.gde.2011.10.004; pmid: 22079435
99. L. D. Landau, E. M. Lifshitz, *Course of Theoretical Physics. Volume 6: Fluid Mechanics* (Butterworth-Heinemann, Oxford, UK, 1987).
100. K. Francis, B. O. Palsson, Effective intercellular communication distances are determined by the relative time constants for cyto/chemokine secretion and diffusion. *Proc. Natl. Acad. Sci. U.S.A.* **94**, 12258–12262 (1997). doi: 10.1073/pnas.94.23.12258; pmid: 9356436


**Acknowledgments:** We thank A. Mitchell, S. Itzkovitz, T. Long, M. Thomson, E. Puchner, K. Roybal, L. Morsut, D. Sivak, A. Raj, and J. Gore for insightful discussions. This work was supported by NIH grants R01 GM55040, R01 GM62583, PN2 EY016546, and P50 GM081879, the NSF Synthetic Biology Engineering Research Center (SynBERC), and the Howard Hughes Medical Institute (HHMI) (to W.A.L.). H.Y. is an HHMI Fellow of the Damon Runyon Cancer Research Foundation (DRG-2089-11).

## Supplementary Materials

www.sciencemag.org/content/343/6171/1242782/suppl/DC1
Materials and Methods
Supplementary Text
Figs. S1 to S23
Tables S1 to S2
References (*101*, *102*)

4 July 2013; accepted 13 December 2013
10.1126/science.1242782